PERGAMON

Vision Research 39 (1999) 2929–2946

Vision Research

Shapes, surfaces and saccades

David Melcher, Eileen Kowler *

Department of Psychology, 152 Frelinghuysen Road, Rutgers University, Piscataway, NJ 08854, USA

Received 22 April 1998; received in revised form 7 January 1999

Abstract

Saccadic localization of spatially extended objects requires the computation of a single saccadic landing position. What representation of the target guides saccades? Saccades were examined for various targets composed of dots to determine whether landing position corresponded to the center-of-gravity (average location) of the dots, the center-of-area of the shape, or the symmetric axis. Targets were composed of dots configured as outline drawings of circles, ellipses, cardioids, wiggly lines, or amorphous blobs. In some cases, dot spacing was varied, extraneous dot clusters were superimposed, or different distributions of dots inside the boundary were added. Quasi-random dot clusters without a well-defined contour were also studied. Instructions were to look at the target as a whole, and keep latency long enough to avoid compromising accuracy. Saccades landed with a high level of precision (S.D.s 7–10% of target eccentricity) near the center-of-area of the target shape, rather than at the center-of-gravity of the dots or on the symmetric axis. Landing position was unaffected by the spacing of dots along the boundary, the addition of dots within the boundary, or the addition of the extraneous dot clusters. When the target was a cluster of quasi-random dots, saccades landed closer to the center-of-area of the implied surface than to the average location of the dots. Overall, the positions of individual dots were important only insofar as the dots affected overall target shape. The results show that a representation of target shape guides saccades, rather than a more primitive representation of individual elements within the attended region.

Keywords: Saccades; Shape; Surfaces; Attention; Eye movement; Localization; Center-of-gravity; Perceptual localization; Symmetric axis

1. Introduction

1.1. The problem

Saccadic localization of objects is nearly as precise as saccadic localization of small target points (Kowler and Blaser, 1995; McGowan, Kowler, Sharma & Chubb, 1998). The high degree of precision is important in natural scenes because there are no markers to flag where, within an object, the saccade should land. Our goal was to find out how a single, precise landing position is derived from visual information extended over space.

1.2. Some relevant background

Oculomotor research has typically avoided the problem of large targets, favoring points, small discs, or crosshairs instead. Nevertheless, there have been several notable exceptions to this general practice, beginning with studies of fixational eye movements in the 1960s. Steinman (1965) tested targets of various sizes and found no effect of target size on either the mean position or the stability of fixation, and concluded that eye position is controlled by a mechanism that averages positional error signals generated at different points along the target's boundary. Kaufman and Richards (1969) and Richards and Kaufman (1969) suggested that shape processing might be involved in fixation control based on their finding that subjects preferred to fixate locations along the symmetric axis of shapes. (The symmetric axis, a 'skeletal' representation of the shape, is the locus of points whose minimal distance from the boundary exists to more than one point along the boundary[1]). But a role for either the symmetric axis,

* Corresponding author.
E-mail address: kowler@rci.rutgers.edu (E. Kowler)

[1] The symmetric axis can be intuitively grasped, as Blum (1973) noted, by imagining a 'grassfire' that starts at the boundary of a shape and burns inward at a constant rate. The points where the grassfire will collapse, and the last embers will burn, form a skeleton of points that are equidistant from the boundary.

0042-6989/99/$ - see front matter
PII: S0042-6989(99)00029-2

shape processing, or spatial averaging in fixation control became unlikely once fixation stability was shown to be independent of target shape (Murphy, Haddad & Steinman, 1974), and dependent on velocity, rather than position, error signals (Epelboim & Kowler, 1993).

The idea that spatial averaging is important in oculomotor control, which originated in the studies of fixation described above, resurfaced later in studies of saccades. Several laboratories found that saccades directed to a target surrounded by nontargets usually landed somewhere near the center of the entire stimulus configuration (Coren & Hoenig, 1972; Findlay, 1982; Ottes, Van Gisbergen & Eggermont, 1985; Cöeffé & O'Regan, 1987). Centering implied that the saccadic error signal is determined by averaging everything in the scene—targets and nontargets alike—but it was hard to know whether this was the best interpretation. For one thing, indiscriminant averaging would produce significant saccadic mislocalizations, something that does not seem to happen in ordinary scanning. Another problem was that saccadic landing position is affected by expectations about where in the target/nontarget configuration the target is likely to appear, which means that centering could have resulted from strategic or attentional factors (He & Kowler, 1989). It seemed that a better way to study averaging, or whatever mechanism is responsible for localizing target objects, would be to use a single spatially-extended target presented without any backgrounds.

1.3. Saccades to spatially-extended targets

Initial studies of saccades to spatially extended targets—outline drawing of simple forms—showed that saccades landed, on average, near the center-of-gravity with a high level of precision regardless of target size (He & Kowler, 1991; Kowler & Blaser, 1995). Saccades made to scan the vertices of a polygon land near the COG of each vertex (Guez, Marchal, Le Gargasson, Grall & O'Regan, 1994).

A well-defined boundary is not necessary in order to achieve precise saccades. McGowan et al. (1998) found that saccades directed to clusters of random dots landed near the center-of-gravity (i.e. average dot location) with the same high level of precision found when targets were outline drawings of simple forms. Saccadic landing position was influenced by local pattern structure in that dots in sparse regions were more influential than dots in dense regions, and bright dots were more influential than dim ones. In contrast, the global structure was unimportant; no extra weight was assigned to dots located near the edges of the pattern or to dots located at smaller retinal eccentricities.

The center-of gravity also provides a reference point for the perceptual localization of clusters of random dots (e.g. Whitaker & Walker, 1988; Morgan, Hole & Glennerster, 1990; Hirsch & Mjolness, 1992) and Gabor patches (Whitaker & McGraw, 1998), although there is evidence for the occasional use of other landmarks, such as edges (Ward, Casco & Watt, 1985) or the midpoint between boundary dots (Badcock, Hess & Dobbins, 1996).

The close proximity of saccadic landing position to the center-of-gravity of dot patterns, and the importance of local, as opposed to global, pattern structure, could be accounted for by a simple model in which saccadic landing position is determined by averaging the local signs of a group of detectors, each centered on a different portion of the attended pattern (McGowan et al., 1998). The contribution of each detector would depend on the number and intensity of elements contained in its 'receptive field', but not on its location relative to other detectors. Thus, according to this model the input to the averaging process is a collection of unrelated elements, not yet assembled into contours, shapes, surfaces or objects.

1.4. Goal of the present paper

The research on saccadic localization summarized above shows that some sort of systematic pooling mechanism is at work to determine the saccadic goal. Notions of pooling have been in the oculomotor literature for some time, but the nature of the information that is pooled remains unknown. Studies using random dot stimuli have suggested that pooling works on a surprisingly primitive representation of the visual target, one that exists prior to the linking of elements into contour and shape, and one that is fundamentally different from the visual scene we perceive when we decide where to look. In the present paper we tested the idea that such a primitive representation is used to guide saccades by using targets whose component elements were not random, but instead configured as shapes with well-defined boundaries.

In the first two experiments target shape was varied to find out whether saccades land at the center of gravity (average location) of the component elements or on the symmetric axis of the shape. Evidence favoring the symmetric axis would imply the involvement of processes sensitive to the relative position of elements, rather than simple averages of element locations. The remaining four experiments investigated the role of target shape using a different approach, namely, varying the spacing of elements on the boundary and the distribution of internal elements to find out whether saccades rely on element- or shape-based representations of the target. Experiments will be described in the order they were run.

2. Experiment 1: symmetric axis versus center-of-gravity

Experiments 1 and 2 were done to determine whether the landing position of saccades was influenced by the symmetric axis of a shape. The experiment was inspired by earlier suggestions of a role for the symmetric axis in fixation control (see Section 1) and by recent psychophysical findings suggesting a role for the symmetric axis in early vision. Kovacs and Julesz (1994) and Kovacs, Feher and Julesz (1998) tested contrast sensitivity for a Gabor patch that was surrounded by a collection of Gabors, including a group arranged as a simple form, such as a circle or an ellipse. Surprisingly, contrast sensitivity was increased when the test patch was located on or near the symmetric axis of a surrounding form. (These authors actually used a D transformation, which is similar to the symmetric axis transformation; see Kovacs et al., 1998, for details.) Contrast sensitivity was highest at the symmetric points of the surrounding form (the points equidistant from the greatest number of boundary locations). If the symmetric axis is extracted at early cortical levels, as these results imply (see also Burbeck & Pizer, 1994), then these landmarks, rather than the center-of-gravity obtained from averaging, might serve as the goal positions of the saccade.

To test the role of the symmetric axis in guiding saccades, landing positions were compared for the following types of targets:

- single dot
- pair of dots separated horizontally
- circle
- ellipse, oriented with the long axis along the horizontal meridian, with an aspect ratio of either 1.2 or 1.4 to 1
- cardioid
- circle fragmented into four arcs.

The symmetric axis of a circle is a single point (symmetric point) and coincides with the center-of-gravity (COG) of the circle. In this paper the COG denotes the average location of all the displayed dots making up the target. The ellipse and the cardioid, in contrast to the circle, have spatially extended symmetric axes (see Fig. 1). If the symmetric axis plays a role in guiding saccades, we expect to find landing positions distributed along the symmetric axis, resulting in an increase in saccadic variability for shapes with extended axes, relative to the variability observed with the circle. Variability should also be greater for the ellipse with the larger aspect ratio (longer symmetric axis). Increased saccadic variability relative to the circle would also be expected with the fragmented circle, which contains many different symmetric axes, varying in size and location. Finally, the fragmented circle, as well as the dot pair, allowed assessment of the importance of a continuous boundary.

2.1. Method

2.1.1. Subjects

The authors were the subjects. DM had normal vision and needed no spectacle correction. A corrective lens was used for EK, who is myopic, in order to maintain a sharp image of the stimulus.

2.1.2. Eye movement recording

Two-dimensional movements of the right eye were recorded by a Generation IV SRI Double Purkinje Image Tracker (Crane & Steele, 1978). The subject's left eye was covered and the head was stabilized on a dental biteboard.

The voltage output of the Tracker was fed on-line through a low pass 50 Hz filter to a 12-bit analog to digital converter (ADC). The ADC, controlled by an IBM compatible PC, sampled eye position every ten ms. The digitized voltages were stored for later analysis.

Tracker noise level was measured with an artificial eye after the tracker had been adjusted so as to have the same first and fourth image reflections as the average subject's eye. Filtering and sampling rate were the same

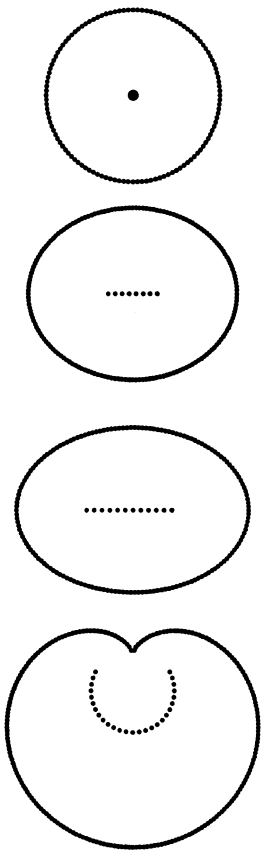

Fig. 1. Four of the target shapes tested (solid lines), along with the corresponding symmetric point (for the circle) or symmetric axis (dotted line). The upper ellipse has an aspect ratio of 1.2:1, and the lower ellipse has an aspect ratio 1.4:1. Neither the symmetric point nor the symmetric axis was displayed during the experiment.

as those used in the experiment. Noise level, expressed as a standard deviation of position samples, was 0.4′ for horizontal and 0.7′ for vertical position.

Recordings were made with the tracker's automatically movable optical stage (auto-stage) and focus-servo disabled. These procedures are necessary with Generation IV Trackers because motion of either the auto-stage or the focus-servo introduces larger artifactual deviations of Tracker output. The focus-servo was used, as needed, only during intertrial intervals to maintain subject alignment. This can be done without introducing artifacts into the recordings or changing the eye position/voltage analog calibration. The auto-stage was permanently disabled because its operation, even during intertrial intervals, changed the eye position/voltage analog calibration.

2.1.3. Stimulus

The stimulus was generated by digital-to-analog converters and shown on a display monitor (Tektronix 608, P4 phosphor) located directly in front of the subject's right eye. The display was refreshed every 20 ms, a rate that was high enough to prevent visible flicker. The luminance of the display, measured by a UDT photometer (model 61) from a 2.2×2.2 cm region containing 1600 points refreshed every 20 ms, was 17 cd/m^2.

The stimuli were seen against a dim (1.8 cd/m^2), homogenous background produced by a raster on a second display monitor located perpendicular to the first. The views of the two displays were combined by a pellicle beam splitter. The combined displays were viewed in a dark room through a collimating lens which placed them at optical infinity.

The background field subtended 20° horizontally by 18° vertically for subject DM and 9.5° horizontally by 7.6° vertically for EK. The difference in background field size was due to the negative lens, placed between the eye and collimating lens, which EK requires to compensate for her myopia and keep the stimuli in sharp focus. The retinal size of the saccadic target, described below, was the same for both subjects.

The target for the saccade was either a single dot, a pair of dots separated by 2°, or one of five shapes (circle, ellipse with aspect ratio set at either 1.2/1 or 1.4/1, cardioid or fragmented circle, see Figs. 1–3). Each shape subtended 2° horizontally at its widest portion. The dots in the first two stimulus types (single dot and dot pair) were made up of a 3×3 array of points, with point separation of 3′. The shapes were made up of single points separated by a distance of 5′.

The eccentricity of the target was either 3.8, 4.0, or 4.2°, where eccentricity was defined as the distance between the center of gravity of the target and the fixation crosshair. The fixation crosshair was displayed 2° to the right of center when leftward eccentricities were tested and 2° to the left of center when rightward eccentricities were tested. This was done so that eye movements would be recorded within the central 5° of the visual field, where tracker output is linear.

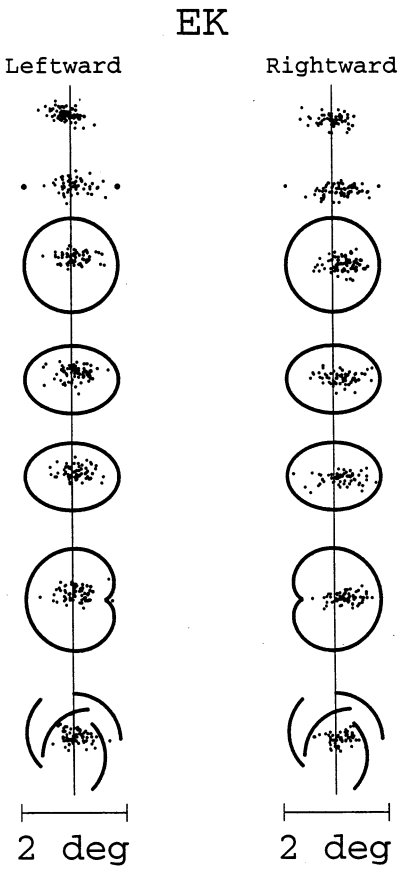

Fig. 2. EK's saccadic landing positions in Experiment 1 for each target type. Leftward and rightward saccades are shown separately. The vertical line connects the horizontal centers-of-gravity (average dot location) of each target. Each dot represents a landing position for the first saccade of one trial.

2.1.4. Procedure

The fixation crosshair was displayed before the start of each trial. The subject started the trial, when ready, with a button press. After a delay of 100 ms, the fixation cross disappeared and the saccadic target was displayed. The stimulus remained on screen for 1900 ms, at which time the trial was over. The direction of the saccade (leftward or rightward of the fixation cross), the eccentricity of the target, and the stimulus type were chosen randomly for each trial. Saccadic direction was disclosed to the subject before the trial by the location of the fixation cross. Eccentricity and target type were not disclosed in advance.

2.1.5. Instructions

The goal of this experiment was to study the spatial properties of saccadic landing positions and relate them to the spatial properties of the stimulus. For this reason instructions to the subject were chosen so as to encour-

age best possible performance and reduce the influence of extraneous behavioral factors that could change saccadic landing positions in ways unrelated to characteristics of the stimulus (He & Kowler, 1991; Kowler & Blaser, 1995).

Subjects were instructed to look at the target as a whole, rather than aim the saccade to a particular place within it. Subjects were also asked to use a single accurate saccade to reach the target and avoid secondary, corrective saccades even if the first seemed to miss the intended goal. The instruction to avoid corrective saccades was used in an attempt to encourage best possible accuracy and discourage a strategy of reaching the target with a sequence of two or more movements.

The subjects were also instructed to adopt relatively long saccadic latencies, the only constraint being to try to complete the saccade before the end of the trial. Long latencies made it more likely that the saccades would be based solely on the target shown in the current trial, rather than be biased toward a location expected to contain the target on the basis of the past history of trials (e.g. Kowler, Martins & Pavel, 1984; Kapoula, 1985).

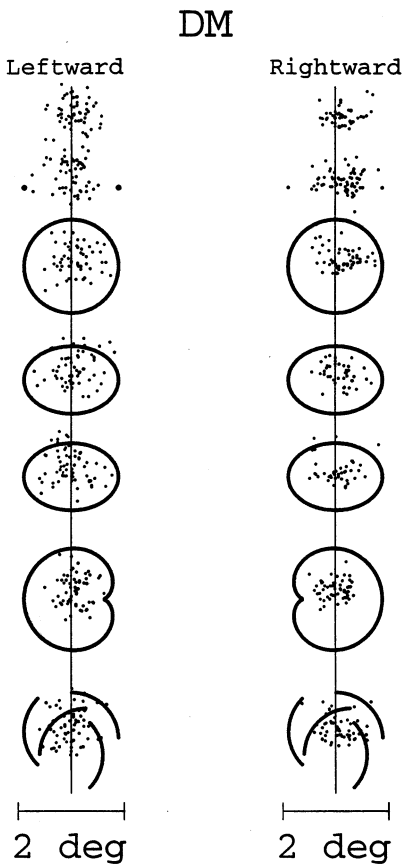

Fig. 3. DM's saccadic landing positions in Experiment 1 for each target type. Leftward and rightward saccades are shown separately. The vertical line connects the horizontal centers-of-gravity (average dot location) of each target. Each dot represents a landing position for the first saccade of one trial.

2.1.6. Detection and measurement of saccades

The beginning and end positions of saccades were detected by means of a computer algorithm employing an acceleration criterion. Specifically, we calculated eye velocity for two overlapping 20 ms intervals. The onset time of the second interval was 10 ms later than the onset time of the first. The criterion for detecting the beginning of a saccade was a velocity difference between the samples of 5°/sec or more. The criterion for saccade termination was more stringent in that two consecutive velocity differences had to be less than 5°/sec. This more stringent criterion was used to ensure that the overshoot at the end of the saccade, which is due in part to movement of the lens during saccades (Crane & Steele, 1978; Deubel & Bridgeman, 1995) and in part to genuine eye movement (Steinman, Haddad, Skavenski & Wyman, 1973; Leigh & Zee, 1991), would be bypassed. The value of the criterion (5°/sec) was determined empirically by examining a large sample of analog records of eye position. Saccades as small as the microsaccades that may be observed during maintained fixation (Steinman et al., 1973) could be reliably detected by the algorithm.

The size of each saccade was defined as the distance between the mean position of the eye at the start of the trial and the position of the eye at the end of the saccade. By using eye position at the start of the trial, rather than eye position at the onset of the detected saccade, our estimate of saccade size also incorporated any pre-saccadic drifts (Kowler & Steinman, 1979) that occurred during the latency interval (drifts were typically $< 10'$ during this interval). The data reported are based on the first saccade of each trial, regardless of whether subsequent saccades occurred.

2.1.7. Number of trials tested and excluded

EK was tested in 11 sessions and DM in eight sessions of 50–100 trials each. Trials were eliminated as follows: trials with latencies less than 100 ms were excluded (EK: 0.4% of trials), since with such short latencies it was unlikely that the stimulus played a significant role in determining the landing position of the saccade. Trials with saccade errors of more than $100'$ (with respect to the center-of-gravity) also were excluded (EK: 1% of trials, DM: 0.6%) because with such large errors the first saccade was not a genuine attempt to reach the target. Trials in which no saccade was made (3.6% of trials for DM) or in which the onset of the first saccade occurred in the last 100 ms (too late to be sure of accurate measurement of saccade offset position) (EK 2.1%, DM: 0.4%) were also excluded. Analyses were based on 916 trials for EK (96%) and 764 trials (96%) for DM.

Table 1
Mean horizontal error relative to center of gravity for targets to the left and right of fixation in Experiment 1 for subjects EK and DM

Subjects	Target	Left				Right			
		Error (min arc)[a]	S.D.[b]	S.D./ecc[c]	N[d]	Error (min arc)[a]	S.D.[b]	S.D./ecc[c]	N[d]
EK	One dot	6.8	13.2	5.5%	79	0.4	15.8	6.6%	57
	Two dots	−2.4	15.6	6.5%	64	9.6	20.2	8.4%	72
	Circle	−3.7	15.6	6.5%	67	15.3	15.4	6.4%	91
	Ellipse 1.2[e]	−4.9	15.3	6.4%	78	9.8	17.4	7.2%	68
	Ellipse 1.4[e]	−4.5	15.2	6.3%	71	11.0	20.4	8.5%	68
	Cardioid	−3.2	17.2	7.2%	67	15.3	16.8	7.0%	65
	Fragmented circle	−1.2	13.4	5.6%	72	5.6	19.3	8.0%	55
DM	One dot	−3.5	17.4	7.3%	53	10.4	16.5	6.6%	46
	Two dots	−1.6	21.4	8.9%	55	9.4	18.8	7.5%	61
	Circle	−6.1	20.7	8.6%	54	10.4	19.7	7.9%	55
	Ellipse 1.2[e]	−5.0	22.0	9.2%	61	6.8	16.6	6.7%	42
	Ellipse 1.4[e]	1.2	20.6	8.6%	62	3.6	19.9	8.2%	41
	Cardioid	−6.0	18.3	7.6%	61	1.3	15.8	6.7%	53
	Fragmented circle	0.7	18.5	7.7%	64	2.9	21.5	8.9%	56

[a] Negative values are undershoots.
[b] S.D., standard deviation.
[c] S.D./ecc, standard deviation divided by eccentricity.
[d] N, number of saccades.
[e] Aspect ratios (1.2:1 or 1.4:1).

2.2. Results

In accordance with instructions, average latencies were long (484 ms for EK; 875 ms for DM) and the vast majority of trials (82% for EK and 93% for DM) contained only a single saccade. Fig. 2 (for EK) and Fig. 3 (for DM) show saccadic landing positions in individual trials for each of the seven target types. The vertical line running down the figures shows the COG of the stimulus elements, i.e. the average horizontal location of all visible points making up the target. Saccades landed near the COG, with average landing position missing the COG by $< 10'$ (see errors relative to the center-of-gravity in Table 1). Saccadic precision was excellent, with standard deviations of about 6–9% of eccentricity for both subjects. Neither the standard deviations, nor mean error relative to the center-of-gravity, differed systematically across the different target types, as shown in Table 1. Standard deviations with the single dot target were slightly smaller than with the other target types.

2.3. Discussion

Landing positions were quite similar for the different target shapes. Both the mean landing position relative to the COG, and the standard deviations of landing position, compared favorably to previous performance reported with single dot or circle targets (Kowler & Blaser, 1995). The standard deviations for the ellipse, cardioid and fragmented circle were not larger than for the circle, despite the extended symmetric axis. The landing positions in the cardioid were not drawn towards the symmetric axis, and the accuracy and precision of saccades to the fragmented circle was about the same as accuracy and precision for the completed circle. Overall, there was no evidence that the symmetric axis contributed to saccadic guidance.

3. Experiment 2: symmetric axis versus center-of-gravity: larger targets and a new shape

The independence of landing position from the symmetric axis was subjected to a stronger test. Larger cardioids were used in order to increase the distance between the center-of-gravity and the symmetric points, and thus increase the likelihood of detecting small deviations in landing position toward these landmarks. The symmetric points for the cardioid are located at the end of the symmetric axis, near the cusps of the cardioid. Also, a new shape was added, the 'yin' (Fig. 4), so named because it is one half of the well-known yin-yang pattern. The yin was tested because, unlike either the cardioid or the ellipse, it has only one symmetric point, which is located at a different place than the center-of-gravity of the boundary points (COG). Also, the 'center-of-area', or COA, of the yin is at a different location than either the COG or the symmetric point. The COA represents the center-of-mass of the shape when it is filled with points of uniform density. It was calculated by filling the shape with points and averaging their location, although such internal points were never actually presented. Also, unlike the ellipse

tested in Experiment 1, the average location of points along the symmetric axis of the yin is different from either the center-of-gravity of the boundary points or the center-of-area. Prior perceptual experiments have shown that subjects tend to locate the perceived center of the yin away from the center-of-gravity of the boundary points and toward the symmetric point (Proffitt, Thomas & O'Brien, 1983).

3.1. Method

Methods were the same as the previous experiment, except as noted below.

3.1.1. Subjects

Subjects EK and DM were tested, along with a naive subject BS. BS had prior experience as an eye movement subject in saccadic experiments, but had no knowledge of the purpose of this experiment.

3.1.2. Stimuli

Targets for saccades were the single dot, circle (diameter 3.5°), cardioid (horizontal extent across the midline = 2.7°; largest vertical extent = 3.45°) and yin. The yins were constructed with respect to either a 3.33 or 6° diameter circumscribed circle (not displayed), so the vertical diameter of the yins (when upright, as in Fig. 4) was equal to the diameter of the circumscribed circle. The yin was displayed in one of three orientations: upright (Fig. 4), or rotated 90° to the right or to the left.

The vertical position of each target shape was randomly chosen on each trial to be either aligned with the horizontal axis or displaced up or down by 0.5°. This was done to discourage a strategy of always looking along the horizontal axis.

3.1.3. Number of trials tested and excluded

Subject EK ran in 14 sessions of 50–100 trials each for a total of 1196 trials. BS and DM each ran in ten sessions of 100 trials. The following trials were excluded: trials with a latency less than 100 ms (BS: 1.2%, EK: 0.2%), saccadic errors greater than 100′ (BS: 1.7%, EK: 0.7%, DM: 4.6%), no detected saccade (one trial for EK), or lost tracker lock (BS: 13%, EK: 3%, DM: 16%). BS's results were based on 837 trials (84% of those tested), DM's on 794 trials (79%), and EK's on 1093 trials (91%).

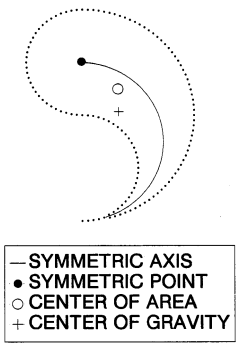

Fig. 4. The yin target along with shape landmarks. The landmarks were not displayed during the experiment.

3.2. Results

Saccades landed at precise locations within these larger shapes. Table 2 shows that horizontal standard deviations were 7–10% of the target eccentricity for EK and BS, and 10–15% for DM.

The increase in target size produced a greater departure of the mean landing position from the COG, with average errors ranging from 1′ to about 60′. Mean landing positions with respect to the COG are shown by the open circles in Figs. 5–7. The displacements from the COG were found even with the target circle, and thus might have originated from processes extraneous to shape analyses or, at the very least, from processes that contributed uniformly across all the shapes. To examine landing positions independently of these influences, an 'adjusted mean landing position' was calculated by subtracting the observed mean deviation from the COG obtained with the target circle from the mean landing position found for each target shape. This adjustment was done separately for each subject and saccadic direction. Consider performance with the cardioids first. The adjusted mean landing positions, shown by the x-symbols in Figs. 5–7, coincided quite closely with the COG for EK and BS. DM's departures from the COG were larger (1–25′) but the saccades were not systematically displaced either towards or away from the symmetric axis.

Results were different for the yin. Figs. 5–7 show that the adjusted mean landing positions did not coincide with the COG, but rather tended to be displaced toward the head of the yin. To look for overall trends, landing positions were plotted on the same graph relative to the boundary of the yin for all 12 yins tested for each subject (two sizes × three orientations × two saccadic directions). To superimpose the yins of different orientations, the shapes were rotated around the COG (the crosshair in Fig. 4). To superimpose the two different sizes, the smaller yins were multiplied by a scale factor of 1.25. The results, plotted in Fig. 8, show that adjusted mean landing positions for BS and EK were displaced above the COG, almost at the center of area (COA) of the surface. DM's adjusted means fell between the COA and the symmetric point.

Table 2
Horizontal S.D. for targets to the left and right of fixation in Experiment 2 for subjects BS, EK, and DM[a]

Subject	Target	Orientation	Left			Right		
			S.D.[c] (min arc)	S.D./ecc[d]	N[b]	S.D.[c] (min arc)	S.D./ecc[d]	N[b]
BS	One dot		23.3	9.7%	41	20.8	8.7%	53
	Circle		25.0	10.4%	32	23.5	9.8%	46
	Small yin	Up	23.4	9.8%	38	23.8	9.9%	46
	Small yin	Right 90°	20.7	8.6%	51	20.7	8.6%	45
	Small yin	Left 90°	19.1	8.0%	33	18.4	7.7%	38
	Cardioid 1	In	15.9	6.6%	28	21.2	8.8%	43
	Cardioid 2	Out	24.3	10.1%	38	25.5	10.6%	58
	Big yin	up	22.8	9.5%	38	22.6	9.4%	36
	Big yin	Left 90°	23.3	9.7%	36	20.7	8.6%	46
	Big yin	Right 90°	21.4	8.9%	36	26.3	11.0%	55
EK	One dot		19.0	7.9%	48	23.9	10.0%	59
	Circle		18.7	7.8%	55	19.1	8.0%	48
	Small yin	Up	14.9	6.2%	66	21.8	9.1%	59
	Small yin	Right 90°	14.7	6.1%	61	19.9	8.3%	55
	Small yin	Left 90°	18.2	7.6%	59	23.1	9.6%	45
	Cardioid 1	In	19.0	7.9%	54	28.2	11.8%	38
	Cardioid 2	Out	16.5	6.9%	58	19.3	8.0%	43
	Big yin	Up	18.3	7.6%	56	25.0	10.4%	69
	Big yin	Left 90°	18.5	7.7%	60	30.5	12.7%	52
	Big yin	Right 90°	16.7	7.0%	47	25.7	10.7%	61
DM	One dot		27.5	11.5%	48	27.3	11.4%	47
	Circle		29.8	12.4%	32	27.7	11.5%	36
	Small yin	Up	26.6	11.1%	48	23.7	9.9%	50
	Small yin	Right 90°	24.2	10.1%	52	41.7	17.4%	12
	Small yin	Left 90°	27.8	11.6%	52	24.6	10.3%	41
	Cardioid 1	In	27.7	11.5%	42	37.1	15.5%	48
	Cardioid 2	Out	36.1	15.0%	52	38.4	16.0%	23
	Big yin	Up	32.4	13.5%	38	25.0	10.4%	52
	Big yin	Left 90°	36.1	15.0%	32	22.3	9.3%	41
	Big yin	Right 90°	17.8	7.4%	37	33.7	14.0%	11

[a] Cardioid 1, corner faces in (towards fixation cross). Cardioid 2, corner faces out (away from fixation cross). Yin stimuli are characterized by size and by the direction that the 'head' (largest part) of the shape is facing, either upright (as in Fig. 4), or tilted 90°.
[b] N, number of saccades.
[c] S.D., standard deviation.
[d] S.D./ecc, standard deviation divided by eccentricity.

3.3. Discussion

The results did not support a role for the symmetric axis in saccadic localization. Landing positions within the cardioid were not displaced toward the symmetric axis and the variability of saccades made to shapes with extended symmetric axes were not greater than the variability of saccades made to the circle.

Performance with the yin was more complex. Mean landing positions for EK and BS coincided well with the center-of-area (COA) of the shape. DM landed somewhere between the symmetric point and the center-of-area, although not on the symmetric axis.

The results with the yin shape are interesting because unlike the other shapes tested, the location of the COG differs from the COA. The possibility that landing position coincides with the COA, which is based on the whole shape, rather than the COG, which is based on the component visible elements, was investigated in the remaining experiments. In these experiments, the dissociation between the COG and COA was increased by varying the spacing of dots along the boundary and by adding dots on and within the boundary.

4. Experiment 3: adding clusters and varying the spacing of points

To further investigate the departures of landing position from the COG of the boundary dots, the yin target was tested again. This time the COG of the dots making up the target was altered by either: (1) adding extraneous dots, or; (2) changing the spacing of dots along the boundary. These transformations altered the COG (average dot location) without changing the overall shape.

4.1. Method

4.1.1. Subjects

The subjects were EK and BS.

4.1.2. Stimuli

Saccadic targets were the circle and the large yins tested in Experiment 2. The yins were once again shown in three different orientations.

Five versions of the yin were tested (Fig. 9). In the first four versions, a dense cluster (diam = 40′, dot separation 5′) of 45 random dots was superimposed on the yin. The dot locations within the cluster were randomly chosen on each trial out of 61 possible locations arranged in a quasi-circular pattern. The dot cluster was superimposed on the yin in one of four locations: two inside the yin, one outside and one on the boundary. These added clusters displaced the COG of the yin from its former value in Experiment 2 by 18′–50′. The fifth version of the yin had no added dot cluster. Instead, the dots making up the boundary in the upper half of the shape were spaced twice as far apart (10′) as the dots in the lower half (5′). Fig. 9 shows the COGs and COAs.

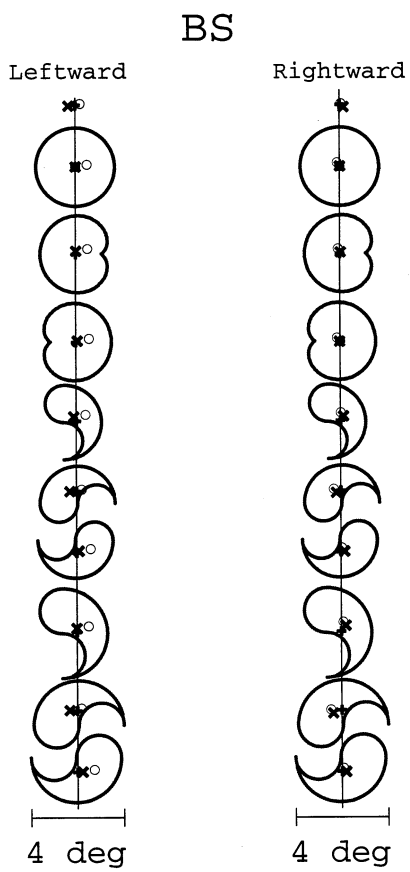

Fig. 5. Mean landing positions (small circles) for BS in Experiment 2. Vertical lines connect the center-of-gravity (average dot location) of each target. The COG is shown by the small crosshair within each target. X's show mean landing position adjusted for the mean under/overshoot observed with circle target. Each mean represents 30–60 trials.

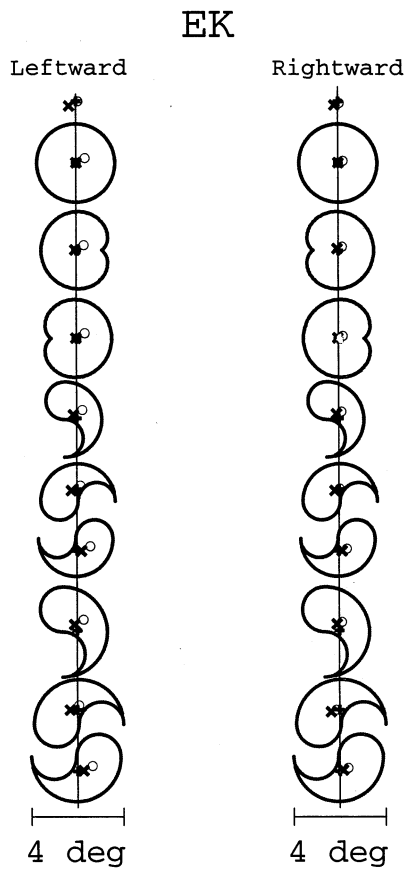

Fig. 6. Mean landing positions (small circles) for EK in Experiment 2. Vertical lines connect the center-of-gravity (average dot location) of each target. The COG is shown by the small crosshair within each target. X's show mean landing position adjusted for the mean under/overshoot observed with circle target. Each mean represents 40–70 trials.

As in the previous experiment, the saccadic target was displaced horizontally (3.8, 4, or 4.2°) and vertically (0, 0.5 up or 0.5° down) relative to the fixation target. These values were calculated as the distance between the fixation cross and the COG of the yin with no added clusters and with the uniform dot spacing. Eccentricity was selected randomly before each trial.

4.1.3. Procedure

The task was identical to the previous two experiments. The only new feature was that when the dot clusters were present, subjects were told to look at the target as a whole and to ignore the added dot clusters. This instruction reduced ambiguity about whether the target was the yin, the dot cluster, or the entire configuration. The type of target presented on each trial (circle or one of the five versions of the yin described above), and the orientation of the target, was chosen randomly and not disclosed to the subject before the target appeared.

4.1.4. Number of trials tested and excluded

Subject BS ran in 18 sessions of 50–100 trials each for a total of 1586 trials. EK ran in 15, 100 trial sessions. The following trials were excluded: trials with a latency less than 100 ms (BS: three trials, EK: two trials), landing errors greater than 100′ (BS: 2%, EK: 1.5%), trials with saccade onset in the final 100 ms of the trial (BS: 7.6%, EK: 0.3%), or lost tracker lock (EK: one trial). BS's results were based on 1430 trials (90% of those tested), EK's on 1471 trials (98%).

4.2. Results

Fig. 9 shows mean landing position, adjusted to compensate for the deviations from the COG observed with the circle, as was done in Experiment 2. Landing positions are shown relative to the boundaries of the yin. Data obtained for each yin orientation and saccadic direction are shown within the same yin.

Saccades landed on average near the center-of-area of the shape, not the center-of-gravity of the dots. Neither the added dot clusters, nor the changes in dot spacing, had systematic effects on mean landing position. Also, the variability of saccades around the means was comparable to that observed with the yin in Experiment 2.

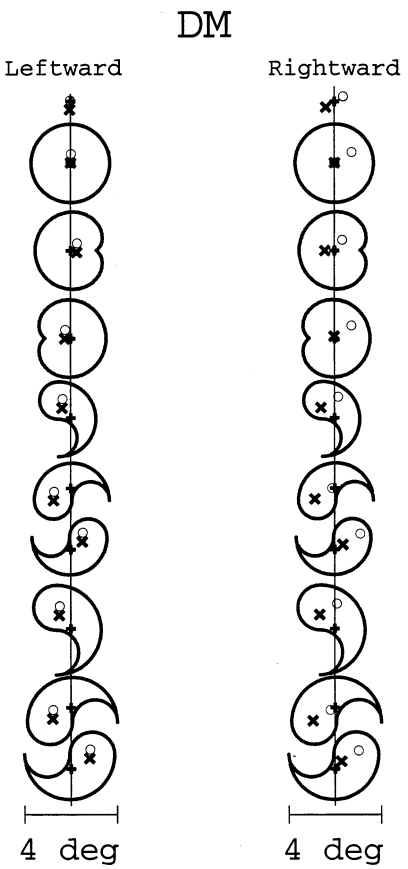

Fig. 7. Mean landing positions (small circles) for DM in Experiment 2. Vertical lines connect the center-of-gravity (average dot location) of each target. The COG is shown by the small crosshair within each target. X's show the mean landing position adjusted for mean under/overshoot observed with circle target. Each mean represents 10–50 trials.

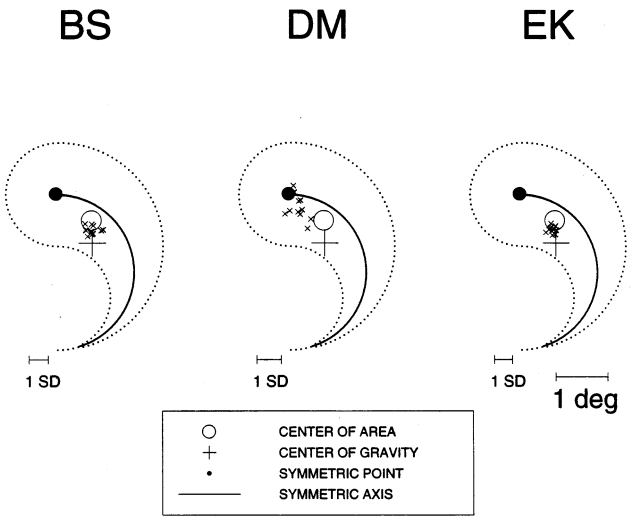

Fig. 8. Mean landing positions for the yin in Experiment 2 adjusted for the mean under/overshoot observed with circle target. The twelve adjusted means (two directions × two sizes × three orientations) are shown by the X's superimposed on a single yin. The error bars indicate average standard deviation for each subject. Shape landmarks are shown, which were not displayed during the experiment.

4.3. Discussion

Saccades landed close to the COA of the yin. Mean landing positions were unaffected by the added dot clusters or by the changes in the spacing of the dots along the boundary. The finding that changes in boundary spacing were irrelevant suggests that saccadic landing position is determined subsequent to the integration of elements into segments of the boundary (Field, Hayes & Hess, 1993; Kovacs & Julesz, 1993; Polat & Sagi, 1994; Kovacs & Julesz, 1994).

The finding that landing positions were unaffected by the superimposed clusters of points argues against indiscriminant pooling of information within a circumscribed spatial region. This result also has implications for the role of attention. Prior work, using concurrent perceptual and saccadic tasks, has shown that attention is allocated to the goal of the saccade shortly before saccadic execution (Hoffman & Subramaniam, 1995; Kowler, Anderson, Dosher & Blaser, 1995). The present results show that differential allocation of attention to the saccadic target is also possible when target (the yin) and background (the superimposed clusters) are located in a common spatial region. This is similar to the ability to smoothly pursue one of two superimposed fields of random dots when the locations of target and background completely overlap (Ter-Braak & Buis, 1970; Neisser & Becklen, 1975; Kowler

et al., 1984; Kowler & Zingale, 1985; Niemann, Ilg & Hoffman, 1994). The attentional selection of the target for eye movements (smooth or saccadic) is occurring at the level of the 'object' rather than the spatial location (Kowler et al., 1984; see Nakayama, He & Shimojo, 1995; Mattingley, Davis & Driver, 1997; for more general treatments of the role of object representations in attention).

5. Experiment 4: variation in element spacing along the contour

Saccadic landing positions in Experiment 3 were unaffected by changes in element spacing on the boundary of the yin. Independence from spacing was confirmed in this experiment using new target shapes and larger differences in the spacing of the component elements.

Two stimulus types were used: a curved line and a blob-like shape (see Figs. 10–12). For both stimuli, the displayed points making up half of the contour were closer together than those making up the other half of the contour. The change in spacing again resulted in a dissociation of the COG of the displayed points and the center-of-area (COA) of the shape.

5.1. Method

5.1.1. Subjects

The subjects were BS, EK and DM.

5.1.2. Stimuli

The squiggly line and the blob-like shape are shown in Figs. 10–12 with the long axes oriented horizontally. In this orientation, the horizontal extent of both the line and blob was 4°. The circle was tested once again to obtain baseline landing positions used to compute the adjusted mean landing positions.

The spacing of the points comprising the boundaries varied within each target. Half the boundary was made up of densely spaced (10′) points and the other half of sparsely spaced points. The sparse spacing was the largest possible that preserved the phenomenal appearance of the overall shape. A spacing of 30′ was used for the blob and a spacing of either 25 or 30′ was used for

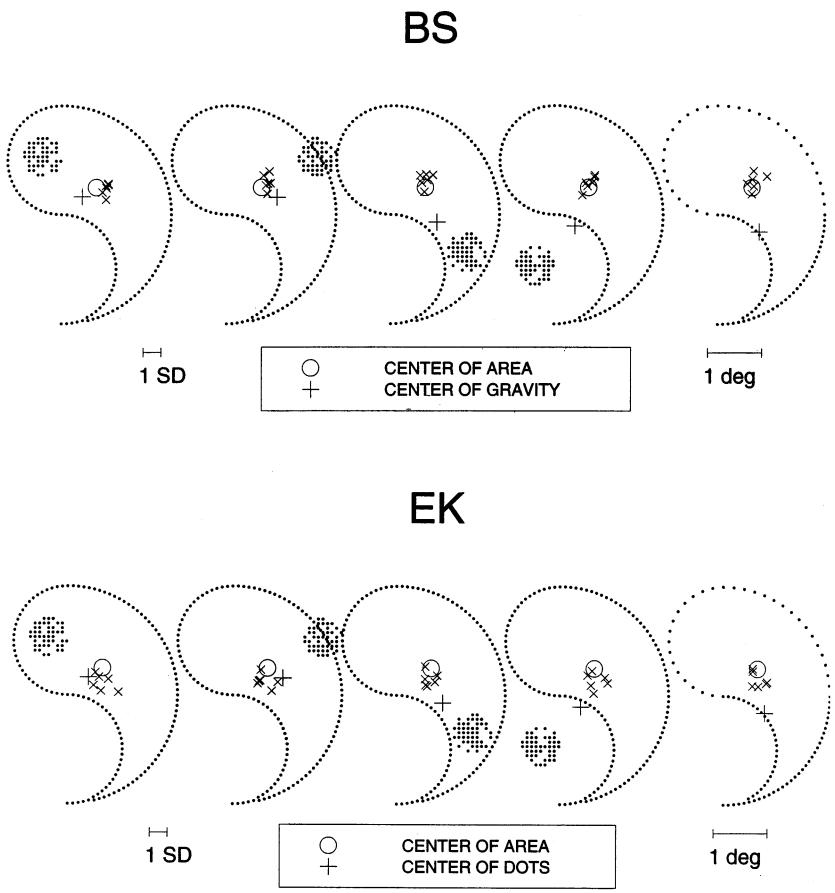

Fig. 9. Mean landing positions (X's) for the yin targets in Experiment 3 adjusted for the mean under/overshoot observed with circle target. Six adjusted means (two directions × three orientations) are shown superimposed on the five types of yin targets tested (four with extraneous dot clusters; one with variable dot spacing). The error bars indicate average standard deviation for each subject. Shape landmarks are shown, which were not displayed during the experiment. Each mean represents 30–60 trials.

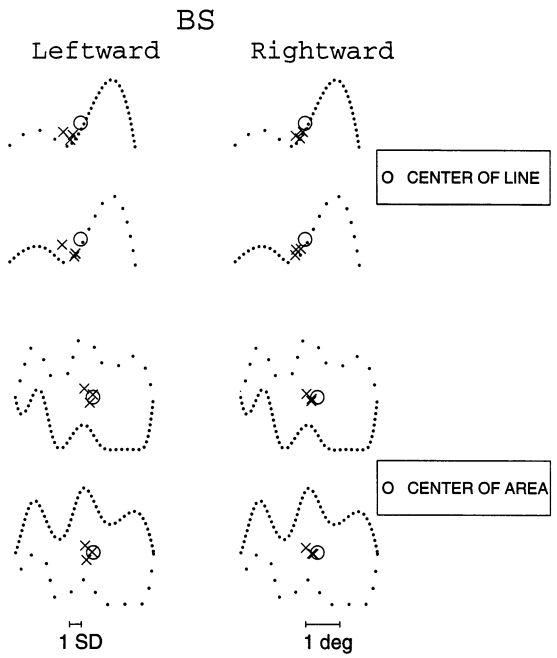

Fig. 10. Mean landing positions (X's) for BS in Experiment 4 adjusted for the mean under/overshoot observed with circle target. Leftward and rightward saccades are shown separately. The three X's in each target were obtained for each of the three orientations tested. The error bars indicate average standard deviation for each subject. Shape landmarks are shown, which were not displayed during the experiment. Means represent 30–70 trials.

the squiggly line (30′ for the portion of the line with the smaller curvature and 25′ for the portion with the larger curvature.)

Two versions of the line and two versions of the blob were created, depending on which side had the more densely spaced points. The difference in the COG between these two versions was 25–30′. Targets were shown in one of three orientations: the long axis aligned with the horizontal meridian, as shown in Figs. 10–12, or rotated by $\pm 90°$. In the horizontal orientation, the densely-spaced portion of the target was either the upper or lower half. In the other orientations, the densely-spaced portion was either on the left or on the right. Target eccentricities, defined with respect to the center-of-areas of the shapes, were the same as in Experiments 2 and 3.

The type of target (circle, blob or line), the spacing of the points, the orientation and the eccentricity were again chosen randomly before each trial. Except for the direction of the saccade, the remaining choices were not disclosed to the subject before the target appeared.

5.1.3. Number of trials tested and excluded

Subject BS ran in 13 sessions, and EK and DM ran in 12 sessions, each containing 100 trials. The following trials were excluded: trials with a latency less than 100 ms (BS: 0.3%, EK: one trial), landing errors greater than 100' (BS: 1.3%., DM: 0.9%, EK: 0.9%), no saccade (BS: 0.5%, DM: 9.5%), lost tracker lock (EK: 0.3%, DM: 0.4%), or saccades occurring in the last 100 ms (BS: 0.3%). BS's results were based on 1268 trials (98% of the trials tested), DM's on 1072 trials (89%), and EK's on 1184 trials (99%) tested.

5.2. Results and Discussion

Mean saccadic landing positions, shown in Figs. 10–12, again adjusted for landing positions obtained with the circle, were in a consistent place near the COA of the blob and near the center of the line regardless of which part of these targets contained densely-spaced points and which contained sparsely-spaced points.

These results confirm and extend the finding in Experiment 3 that spacing of points making up the contour does not affect saccadic landing position and that landing position is best predicted by the center-of-area of the shape. This is further evidence that the spatial pooling process determining saccadic landing position occurs subsequent to the integration of elements into contours and the generation of surface shape.

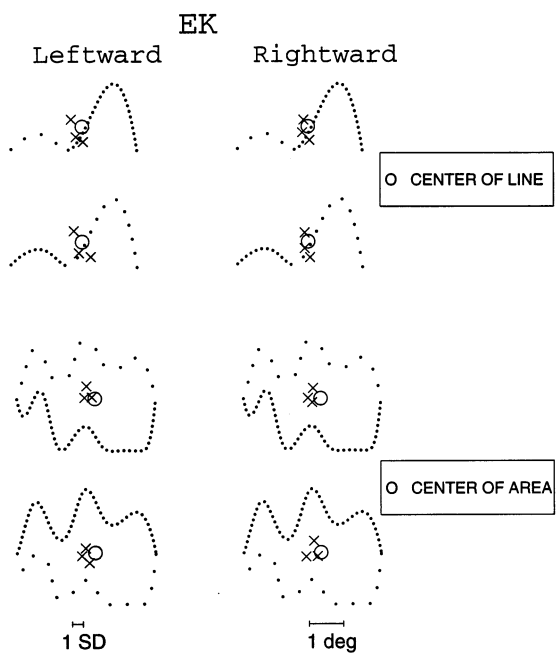

Fig. 11. Mean landing positions (X's) for EK in Experiment 4 adjusted for the mean under/overshoot observed with circle target. Leftward and rightward saccades are shown separately. The three X's in each target were obtained for each of the three orientations tested. The error bars indicate average standard deviation for each subject. Shape landmarks are shown, which were not displayed during the experiment. Means represent 30–60 trials.

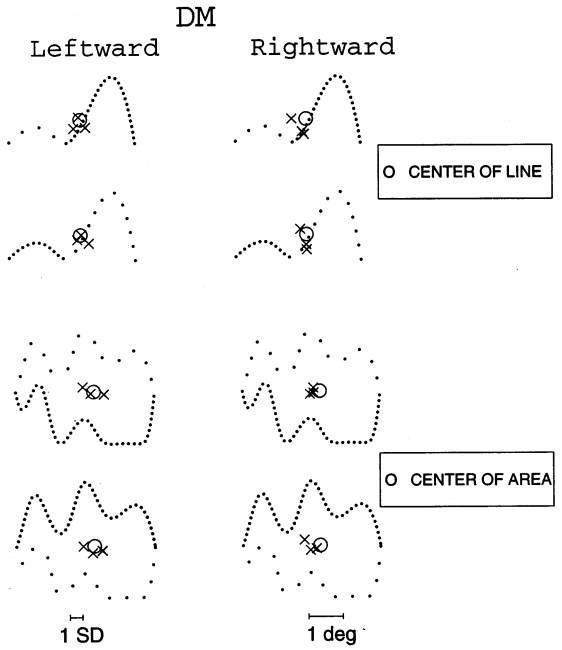

Fig. 12. Mean landing positions (X's) for DM in Experiment 4 adjusted for the mean under/overshoot observed with circle target. Leftward and rightward saccades are shown separately. The three X's in each target were obtained for each of the three orientations tested. The error bars indicate average standard deviation for each subject. Shape landmarks are shown, which were not displayed during the experiment. Means represent 30–60 trials.

6. Experiment 5: adding internal elements

In this experiment, internal dots were added within the boundaries of a new blob-like shape. The density of the internal dots was varied randomly according to one of two ramp functions. As in the previous experiment, this transformation changes the center-of-gravity of the elements (COG) without changing the center-of-area of the shape (COA).

6.1. Method

6.1.1. Subjects

Subjects were BS, DM, and EK.

6.1.2. Stimuli

Targets were 'blob'-like shapes with a long-axis of 4° (see Fig. 13). Not all dots on the boundary were displayed. To determine which dots on the boundary would be displayed, the boundary was divided into locations spaced 10′ apart and the probability of a dot being displayed in any location was 0.9. The removal of these few dots did not perturb the overall perceived shape.

Dots were generated inside the contour according to the following algorithm. The blob oriented with the long axis horizontal was divided into columns and rows of possible locations (separation = 10′). On half of the trials (chosen randomly), the probability that a particular location was filled in any column was chosen according to a ramp function that decreased from a probability of 0.9 in the leftmost columns to 0.3 in the rightmost column. On the rest of the trials the slope of the ramp was reversed, creating the opposite probability distribution.

As a result of the addition of the internal dots, the COG (average dot location) was on average 20′ away from the COA and the difference in COGs between targets generated according to the two probability ramps was 40′.

As in the previous experiment, the blobs were randomly displayed in three different orientations. A circle with diameter of 3.5° was also tested. Eccentricities were the same as those in Experiments 2–4 and, as in Experiment 4, defined with respect to center-of-area, ignoring the presence of the internal elements. The type of target (circle or blob), the distribution of internal dots within the blob, and the orientation and the eccentricity of the target were again chosen randomly before each trial. Except for the direction of the saccade, the remaining choices were not disclosed to the subject before the target appeared.

6.1.3. Number of trials tested and excluded

Subjects BS, EK and DM each ran in four sessions of 100 trials. The following trials were excluded: landing errors greater than 100′ (BS: 1.0%., EK: 1.0%, DM: one trial), no saccade (DM: 1.5%), or lost tracker lock (EK: one trial, BS: one trial). BS's results were based on 395

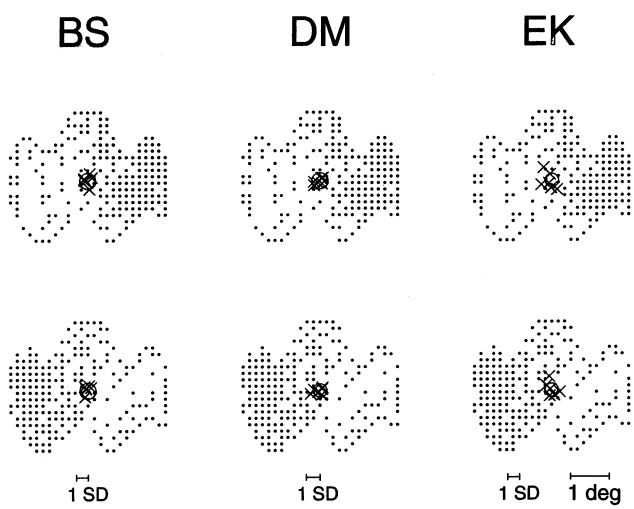

Fig. 13. Mean landing positions (X's) adjusted for the mean under/overshoot observed with circle target in Experiment 5. Performance is shown separately when dots were more probable on the right (top) and on the left (bottom). These targets are illustrative; actual dot locations were randomly chosen in the experiment according to a ramp function (see text). Six X's are shown per subject (two directions × three orientations). Error bars indicate average standard deviations for each subject. Shape landmarks are shown, which were not displayed in the experiment. Means represent 30–50 trials.

trials (99% of those tested), DM's on 393 trials (98%), and EK's on 395 trials (99%).

6.2. Results and discussion

The addition of internal dots did not affect saccadic landing position. The mean adjusted landing positions, shown in Fig. 13, collapsed over orientation and saccadic direction, coincided well with the center-of-area of the shape. This provides further evidence that target shape, rather than the position of individual elements, determines saccadic landing position. Findlay, Brogan and Wenban-Smith (1993) argued for the importance of boundaries, as opposed to internal elements, based on their study of biases introduced in saccadic landing position by a pair of stimuli (checkerboard and checkerboard frame) flashed during the saccadic programming interval. Given our finding that spacing of elements composing the boundary did not affect landing position (Experiments 3 and 4, above), saccades appear to be guided by representations of overall target shape, rather than by the positions of the individual boundary elements.

7. Experiment 6: random dots revisited

The results so far show that saccades land at the center of area of the shape, rather than at the center of gravity of the displayed elements. Large changes in element density, which altered the COG, did not affect saccades. By contrast, prior work using random dot patterns supported the importance of the center-of-gravity of the elements in both saccadic (McGowan et al., 1998) and perceptual (Whitaker & Walker, 1988; Morgan et al., 1990; Hirsch & Mjolness, 1992) localization.

This experiment tested whether differences between our results and prior results obtained with random dot patterns might have been due to the particular choice of stimulus elements, or to some other aspect of the display.

The target was a quasi-random pattern of dots. Dot locations were selected by random perturbations of the locations of points making up blob patterns similar to those studied in Experiment 5. As in Experiment 5, a probability ramp was used to choose the location of displayed dots. Unlike Experiment 5, the probability of displaying a contour dot was not greater than that of displaying an internal dot. Also, dot locations were jittered to disrupt the appearance of a continuous boundary. These perturbations were imposed on four differently-shaped arrays of possible dot locations to increase the heterogeneity of the stimulus set.

7.1. Method

7.1.1. Subjects

BS, EK and DM were the subjects. They had different levels of knowledge about the experiment. BS was naive to the purpose of the entire project. EK knew that quasi-random dot clusters would be displayed, but was unaware of the algorithm used to generate the targets, or the shape of the arrays of possible dots. DM knew the grid shapes and the algorithm for creating the display, but had not seen the particular stimuli that were displayed on individual trials, because stimuli were generated by a computer algorithm, described below.

7.1.2. Stimuli

Four different dot grids were created, with each grid representing the set of possible locations from which the displayed dots would be selected. The first grid was identical to the blob shape in Experiment 5; the second grid had an ellipsoidal shape, and the third and fourth grids were $4 \times 2°$ rectangles. The spacing between elements in the first three grids was $10'$, and the spacing in the fourth was $20'$.

The grid was divided into 12 columns. To select the locations that would contain displayed dots, one of two probability ramps was first applied in which the probability of displaying a location decreased from 0.9 in the left-hand (right-hand) column to 0.3 in the right-hand (left-hand) column. A random vertical jitter was then added to each column. For grid shapes one and three (see preceding paragraph for the shape descriptions), the jitter of each column was independently selected to be in the range of 0–1°. For grids two and four, the range was 0–1.2°. The vertical and horizontal extent of the stimuli was constrained to not exceed 4°. The set of dots was rotated either 0, or $\pm 90°$, as in Experiment 5. As a final step, the entire cluster of dots was positioned so that the center-of-gravity (average dot location) was either 3.8, 4.0, or 4.2° horizontally and either 0, 0.5° down or 0.5° up vertically. The circle target was not re-tested. Data obtained from the circle in Experiment 5 was used to compute the adjusted mean landing positions. Fig. 14 shows examples of targets for each of the four types of grid shapes. The target configuration and eccentricity were chosen randomly before each trial and, except for the direction of the saccade, not disclosed to the subject before the target appeared.

7.1.3. Determining the implied surface

In order to compare the center-of-gravity of the stimulus elements to the center-of-area of an implied surface shape, a uniform surface representation was created by filling empty spaces in the matrix of possible (x, y) locations. This was done by first finding the maximum and minimum values of y in each column. Then, an array of dots, separated by $10'$, was generated

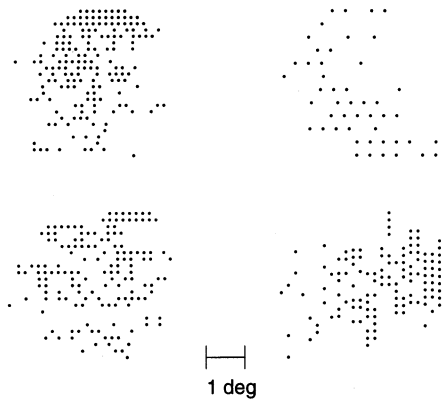

Fig. 14. Examples of quasi-random dot targets used in Experiment 6.

between the maximum and minimum value of y. The center-of-area was calculated as the average location of all the dots in the filled-in implied surface. The distance between the COG and COA, averaged over all targets generated, was 14′.

7.1.4. Number of trials tested and excluded

Subject EK ran in nine sessions and BS and DM in eight sessions of 100 trials. The following trials were excluded: trials with a latency less than 100 ms (BS: 0.4%, EK: 0.2%), landing errors greater than 100′ (BS: 3.1%, DM: 1.0%, EK: 0.7%), no saccade (BS: 0.4%, DM: 2.4%, EK: one trial), or lost tracker lock (EK: 0.3%). BS's results were based on 769 trials (96% of trials tested), DM's on 773 trials (97%), and EK's on 888 trials (99%).

7.2. Results

Saccadic landing positions were first analyzed with respect to the COG of the displayed points in order to compare these results to previous work. Mean adjusted landing positions were near the COG. Average error with respect to the COG, shown in Table 3, was small,

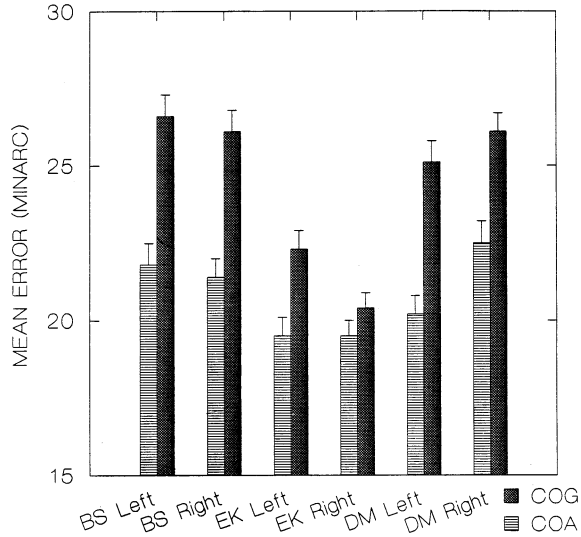

Fig. 15. Mean vector error with respect to center-of-gravity (average dot location) (COG) and center of area (COA) for each subject and saccadic direction in Experiment 6. Each bar represents approximately 400 trials. Error bars indicate standard error. The mean vector difference between the COA and COG of the targets was 12 min arc.

usually $< 15'$. Standard deviations of landing positions around the COG were 7–10% of eccentricity. These mean errors and standard deviations were similar to those reported in McGowan et al. (1998) for random arrays of dots. This correspondence shows that the predominance of shape over dots observed in the present study was not likely to be due to differences in the nature of the dots themselves.

Landing positions were close to the COG of the dots, but closer still to the COA of the inferred shape. Fig. 15 shows that mean vector errors relative to the center-of-area of the implied, filled-in surface were smaller than mean vector errors relative to the center-of-gravity of the displayed dots. The differences between mean vector errors for these two landmarks were smallest for subject EK.

Table 3
Mean horizontal and vertical error relative to center of gravity for targets to the left and right of fixation in Experiment 6 for subjects BS, EK, and DM

Subject	Left					Right				
	Horizontal		Vertical		N[b]	Horizontal		Vertical		N[b]
	Error (min arc)[a]	S.D./ecc[c]	Error (min arc)[a]	S.D./ecc[c]		Error(min arc)	S.D./ecc[c]	Error (min arc)[a]	S.D./ecc[c]	
BS	−8.9	9.4%	13.2	8.3%	368	0.0	9.3%	−0.4	8.0%	401
EK	−12.6	8.3%	−0.4	6.6%	428	4.3	7.1%	−3.1	6.7%	460
DM	−1.1	8.6%	23.4	8.0%	374	4.3	10.4%	13.2	7.1%	399

[a] Negative values indicate undershoots.
[b] Number of saccades.
[c] S.D./ecc, standard deviation divided by eccentricity.

Mean vector errors were compared to those obtained in Experiment 5, where the shape of the implied surface was more apparent (Fig. 13) than that of the randomly-generated dots (Fig. 14). Mean vector error relative to the COA was the same (21′ averaged across subjects and directions). Mean vector error relative to the COG was larger for the well-defined shapes of Experiment 5 (30′) than for the random dots of Experiment 6 (24′). These larger errors for Experiment 5 most likely were due to the greater difference between the COG and COA of the shapes rather than any difference in processing the two kinds of targets.

7.3. Discussion

Saccades landed closer to the center-of-area of the estimated shape than to the average dot location, even for quasi-random arrays of dots.

McGowan et al. (1998) tested patterns in which dots were randomly scattered in a circular region. They found that saccadic landing position was close to the COG (average dot location) with no extra weight assigned to dots near the edges, but with dots in sparse locations having more influence than dots in dense locations. This effect of density could have resulted from purely local events, for example, the response of a detector centered on different local regions increasing at a successively slower rate with increasing numbers of dots in its 'receptive field'. But the importance of shape, in contrast to dots, found with the quasi-random patterns in the present study suggests an alternative explanation, namely, dots in sparse regions were more important than dots in dense regions because a uniform surface is imposed over the field of random dots before saccadic landing position was determined.

8. Conclusions and implications

The results of the six experiments resolve questions about the visual representations used to guide saccades. We found that saccades directed to a variety of simple shapes land closer to the center-of-area of a 'filled-in' shape than to the average location of the visible elements making up the shape. Neither changes in the density of elements making up the boundary, nor the addition of different patterns of elements inside the boundary, affected landing position, even though the positions of the component elements were clearly discriminable in the eccentric targets. The symmetric axis of the shape, which may be extracted at early levels of visual analysis based on local interactions across the boundaries, was not influential. Taken together, the results show that saccades are guided by an abstract representation of the shape, which transcends the local distribution of elements.

The high level of saccadic precision (standard deviations of landing positions $< 10\%$ of eccentricity), comparable to those obtained in prior experiments with a variety of target configurations, including single points (see Section 1), attests to the systematic nature of the process used to determine landing position. The precision of coding the location of the target is not compromised by use of a higher-order representation of shape, as opposed to representations of visible elements.

The finding that saccadic landing positions are based on the shape of the target was obtained under the instructions to look at the target as a whole and to adopt saccadic latencies that seemed long enough to avoid compromising accuracy. Under these conditions, there should be ample time to allow shape construction, as well as equal attentional weighting throughout the target and attentional suppression of any non-target distractors (Experiment 3). What if less time were available? Under such conditions, the visual representation guiding saccades might differ (for a discussion of temporal factors in perceptual representation, see Burbeck, 1986; Watt, 1987; Pizlo, Rosenfeld & Epelboim, 1995). Various ways to reduce processing time, however, introduce extraneous behavioral factors that would complicate the interpretation of results. For example, reducing saccadic latencies can invoke a speed/accuracy tradeoff, in which saccadic landing positions are biased according to past history of the target locations (Kowler et al., 1984; Kapoula, 1985; He & Kowler, 1989). Using very brief target presentations can impair accuracy and also increase reliance on memory (Aitsebaomo & Bedell, 1992). Finally, rapid sequences of saccades during natural scanning are affected by strategies and attentional allocation depending upon the particular scanning task. All these extraneous factors, introduced when different methods of reducing processing time are adopted, would have to be taken into account in order to correctly characterize the visual representation available to saccades. Our results show that under conditions designed to produce best possible accuracy and precision, visual information up to the level of shape construction is used by the saccadic system.

One implication of the finding that saccades can be guided by shape is that saccades may prove to be a useful tool in testing models of how shape is generated from collections of component elements. Saccadic landing positions may be particularly useful in resolving questions about the rules applied by the visual system to link component elements into shapes (Feldman, 1997) or to segregate groups of elements from backgrounds (Field et al., 1993; Pizlo, Salach-Golyska & Rosenfeld, 1997). Saccadic landing positions in ambiguous situations could disclose which of several possible structures is preferred by the visual system.

The success of attempts to link saccades to models of shape generation will depend on the extent to which

subsequent studies can show that saccadic landing position coincides with the center-of-area of targets whose shape is unambiguous. We feel it is necessary to be cautious about predicting such an outcome because shape provides, at most, a vehicle to guide saccades under instructions to look at the target object as a whole. Looking at the whole object appears to be what people do when scanning naturally (they don't select which letter in a word, or which portion of the coffee cup, to look at). Nevertheless, landing positions other than the center can be attained if subjects so choose (He & Kowler, 1991), presumably by shifting the distribution of attention applied to the target (Kowler et al., 1995; Hoffman & Subramaniam, 1995). We found evidence of such flexibility of landing position in subject DM's performance in Experiment 2 with the yin shape, where his landing positions missed all the expected landmarks (Fig. 8). In such cases selected regions or local features of the form may play a role. Evidence for use of spatially local cues has appeared in studies of perceptual localization of dot patterns as well (Ward et al., 1985; Badcock et al., 1996). The ability to steer the saccade to locations other than the 'default' center-of-area may be essential if saccades are to be useful in natural scanning.

The precise and accurate saccades observed in this and in prior work, obtained with no special effort on the part of the subject other than the attempt to look at the whole target, show that the oculomotor system is not contributing either excessive noise or systematic errors, but is supplying a stable platform against which cognitive decisions can be effective in displacing landing position from the center, depending on the demands of the particular task. Given that natural viewing conditions are characterized by inconsistent lighting and viewing angle, basing saccadic localization on a representation of target shape, rather than component elements, ensures consistent landing positions tied to important aspects of the target rather than to irrelevant fluctuations in internal details. Landing at the center of the shape produces equivalent visual resolution for boundaries across the whole shape. The center may be the best vantage point for overall object recognition.

Acknowledgements

The research was supported by a grant from the Air Force Office of Scientific Research, Program on Spatial Orientation, F49620-96-1-0081. DM was supported in part by AASERT grant AFOSR F49620-93-1-0408. We thank Ilona Kovacs and Akos Feher for helpful comments during the course of this research, including the suggestion to use the yin shape in Experiments 2 and 3. We also thank Jacob Feldman and Thomas Papathomas for comments on the work, and BS for dedicated service as a subject.

References

Aitsebaomo, A. P., & Bedell, H. E. (1992). Psychophysical and saccadic information about direction for briefly presented visual targets. *Vision Research*, *32*, 1729–1737.

Badcock, D. R., Hess, R. F., & Dobbins, K. (1996). Localization of element clusters: multiple cues. *Vision Research*, *36*, 1467–1472.

Blum, H. (1973). Biological shape and visual science (part I). *Journal of Theoretical Biology*, *38*, 205–287.

Burbeck, C. A. (1986). Exposure-duration effects in localization judgements. *Journal of the Optical Society of America A*, *3*, 1983–1988.

Burbeck, C. A., & Pizer, S. M. (1994). Object representation by cores: Identifying and representing primitive spatial regions. *Vision Research*, *35*, 1917–1930.

Cöeffé, C., & O'Regan, J. K. (1987). Reducing the influence of non-target stimuli on saccade accuracy: predictability and latency effects. *Vision Research*, *27*, 227–240.

Coren, S., & Hoenig, P. (1972). Effect of non-target stimuli upon length of voluntary saccades. *Perceptual and Motor Skills*, *34*, 499–508.

Crane, H. D., & Steele, C. S. (1978). Accurate three-dimensional eyetracker. *Applied Optics*, *17*, 691–705.

Deubel, H., & Bridgeman, B. (1995). Fourth Purkinje image signals reveal eye-lens deviations and retinal image distortions during saccades. *Vision Research*, *35*, 529–538.

Epelboim, J., & Kowler, E. (1993). Slow control with eccentric targets: evidence against a position-corrective model. *Vision Research*, *33*, 361–380.

Feldman, J. (1997). Curvilinearity, covariance, and regularity in perceptual groups. *Vision Research*, *37*, 2835–2848.

Field, D. J., Hayes, A., & Hess, R. F. (1993). Contour integration by the human visual system: evidence for a local 'association field'. *Vision Research*, *33*, 173–193.

Findlay, J. M. (1982). Global visual processing for saccadic eye movements. *Vision Research*, *22*, 1033–1045.

Findlay, J. M., Brogan, D., & Wenban-Smith, M. G. (1993). The spatial signal for saccadic eye movements emphasizes visual boundaries. *Perception and Psychophysics*, *53*, 633–641.

Guez, J., Marchal, P., Le Gargasson, J., Grall, Y, & O'Regan, J. K. (1994). Eye fixations near corners: evidence for a centre of gravity calculation based on contrast, rather than luminance or curvature. *Vision Research*, *34*, 1625–1635.

He, P., & Kowler, E. (1989). The role of location probability in the programming of saccades: Implications for 'center of gravity' tendencies. *Vision Research*, *9*, 1165–1181.

He, P., & Kowler, E. (1991). Saccadic localization of eccentric forms. *Journal of the Optical Society of America A*, *8*, 440–449.

Hirsch, J., & Mjolness, E. (1992). A center-of-mass computation describes the precision of random dot displacement discrimination. *Vision Research*, *32*, 335–346.

Hoffman, J., & Subramaniam, B. (1995). The role of visual attention in saccadic eye movements. *Perception and Psychophysics*, *57*, 787–795.

Kaufman, L., & Richards, W. (1969). Spontaneous fixation tendencies for visual forms. *Perception and Psychophysics*, *5*, 85–88.

Kapoula, Z. (1985). Evidence for a range effect in the saccadic system. *Vision Research*, *25*, 1155–1157.

Kovacs, I., & Julesz, B. (1993). A closed curve is much more than an incomplete one: effect of closure in figure-ground segmentation. *Procedures of the National Academy of Sciences, USA*, *90*, 7495–7497.

Kovacs, I., & Julesz, B. (1994). Perceptual sensitivity maps within globally defined visual shapes. *Nature*, *370*, 644–646.

Kovacs, I., Feher, A., & Julesz, B. (1998). Medial-point description of shape: a representation for action coding and its psychophysical correlates. *Vision Research*, *38*, 2323–2333.

Kowler, E., Anderson, E., Dosher, B., & Blaser, E. (1995). The role of attention in the programming of saccades. *Vision Research*, *35*, 1897–1916.

Kowler, E., & Blaser, E. (1995). The accuracy and precision of saccades to small and large targets. *Vision Research*, *12*, 1741–1754.

Kowler, E., Martins, A. J., & Pavel, M. (1984). The effect of expectations on slow oculomotor control- IV: anticipatory smooth eye movements depend on prior target motions. *Vision Research*, *24*, 197–210.

Kowler, E., & Steinman, R. M. (1979). The effect of expectations on slow oculomotor control- II. Single target displacements. *Vision Research*, *19*, 633–646.

Kowler, E., & Zingale, C. (1985). Smooth eye movements as indicators of selective attention. In M. I. Posner, & O. S. M. Marin, *Attention and performance XI* (pp. 285–300). Hillsdale, New Jersey: Lawrence Erlbaum Associates Inc.

Leigh, R. J., & Zee, D. S. (1991). *The Neurobiology of Eye Movements* (2nd ed.),(pp. 82). Philadelphia: F. A. Davis

Mattingley, J. B., Davis, G., & Driver, J. (1997). Pre-attentive filling-in of visual surfaces in parietal extinction. *Science*, *275*, 671–674.

McGowan, J., Kowler, E., Sharma, A., & Chubb, C. (1998). Saccadic localization of random dot targets. *Vision Research*, *38*, 895–909.

Morgan, M. J., Hole, G. J., & Glennerster, A. (1990). Biases and sensitivities in geometrical illusions. *Vision Research*, *30*, 1793–1810.

Murphy, B. J., Haddad, G. M., & Steinman, R. M. (1974). Simple forms and fluctuations of the line of sight: Implications for motor theories of form processing. *Perception and Psychophysics*, *16*, 557–563.

Nakayama, K., He, Z. J., & Shimojo, S. (1995). Visual surface representation: a critical link between lower-level and higher-level vision. In S. M. Kosslyn, & D. N. Osherson, *Introduction to cognitive science: visual cognition* (pp. 1–70). Cambridge, MA: MIT Press.

Neisser, U., & Becklen, R. (1975). Selective looking: attending to visually specific events. *Cognitive Psychology*, *7*, 480–494.

Niemann, T., Ilg, U. J., & Hoffman, K. P. (1994). Eye movements elicited by transparent stimuli. *Experimental Brain Research*, *98*, 314–322.

Ottes, F. P., Van Gisbergen, J. A. M., & Eggermont, J. J. (1985). Latency dependence of colour-based target versus non-target discrimination by the saccadic system. *Vision Research*, *25*, 849–862.

Polat, U., & Sagi, D. (1994). The architecture of perceptual spatial interactions. *Vision Research*, *34*, 73–78.

Pizlo, Z., Rosenfeld, A., & Epelboim, J. (1995). An exponential pyramid model of the time-course of size processing. *Vision Research*, *35*, 1089–1107.

Pizlo, Z., Salach-Golyska, M., & Rosenfeld, A. (1997). Curve detection in a noisy image. *Vision Research*, *37*, 1217–1241.

Proffitt, D. R., Thomas, M. A., & O'Brien, R. G. (1983). The role of contour and luminance distribution in determining perceived centers within shapes. *Perception and Psychophysics*, *33*, 63–71.

Richards, W., & Kaufman, L. (1969). 'Center of gravity' tendencies for fixations and flow patterns. *Perception and Psychophysics*, *5*, 81–84.

Steinman, R. M. (1965). Effects of target size, luminance, and color on monocular fixation. *Journal of the Optical Society of America*, *55*, 1158–1165.

Steinman, R. M., Haddad, G. M., Skavenski, A. A., & Wyman, D. (1973). Minitiature eye movements. *Science*, *181*, 810–819.

TerBraak, J. W. G., & Buis, C. (1970). Optokinetic nystagmus and attention. *International Journal of Neurology*, *8*, 34–42.

Ward, R. M., Casco, C., & Watt, R. J. (1985). The location of noisy visual stimuli. *Canadian Journal of Psychology*, *39*, 387–399.

Watt, R. J. (1987). Scanning from coarse to fine spatial scales in the human visual system after the onset of a stimulus. *Journal of the Optical Society of America*, *4*, 2006–2021.

Whitaker, D., & Walker, H. (1988). Centroid evaluation in the vernier alignment of random dot clusters. *Vision Research*, *7*, 777–784.

Whitaker, D., & McGraw, P. V. (1998). The effect of suprathreshold contrast on stimulus centroid and its implications for the perceived location of objects. *Vision Research*, *38*, 3591–3599.